Reconciling Atmospheric and Oceanic Views of the Transient Climate Response to Emissions

Anna Katavouta[1*], Richard G. Williams[1*], Philip Goodwin[2] and Vassil M. Roussenov[1]

Anna Katavouta and Richard G. Williams, a.katavouta@liverpool.ac.uk and ric@liverpool.ac.uk

[1]Department of Earth Ocean and Ecological Sciences, University of Liverpool, Liverpool, UK

[2]School of Ocean and Earth Sciences, University of Southampton, Southampton, UK

This article has been accepted for publication and undergone full peer review but has not been through the copyediting, typesetting, pagination and proofreading process, which may lead to differences between this version and the Version of Record. Please cite this article as doi: 10.1029/2018GL077849

The Transient Climate Response to Emissions (TCRE), the ratio of surface warming and cumulative carbon emissions, is controlled by a product of thermal and carbon contributions. The carbon contribution involves the airborne fraction and the ratio of ocean saturated and atmospheric carbon inventories, with this ratio controlled by ocean carbonate chemistry. The evolution of the carbon contribution to the TCRE is illustrated in a hierarchy of models: a box model of the atmosphere-ocean and an Earth system model, both integrated for 1000 years, and a suite of Earth system models integrated for 140 years. For all models, there is the same generic carbonate chemistry response: an acidifying ocean during emissions leads to a decrease in the ratio of the ocean saturated and atmospheric carbon inventories, and the carbon contribution to the TCRE. Hence, ocean carbonate chemistry is important in controlling the magnitude of the TCRE and its evolution in time.

Keypoints:

- Transient climate response to emissions (TCRE) depends on the product of thermal and carbon contributions that need not exactly compensate.
- The carbon contribution to the TCRE depends on the airborne fraction and the ratio of the ocean carbon saturation and atmospheric carbon.
- An acidifying ocean decreases the ratio of ocean carbon saturation and atmospheric carbon, and so the carbon contribution to the TCRE.

1. Introduction

Climate model projections reveal that surface global warming is nearly proportional to the cumulative carbon emission [*Allen et al.*, 2009; *Matthews et al.*, 2009; *Zickfeld et al.*, 2009; *Gillet et al.*, 2013]. This relationship is encapsulated in the near constancy of an empirical climate metric, the Transient Climate Response to cumulative carbon Emissions (TCRE), which is defined by the ratio of the change in global-mean, surface air temperature since the pre-industrial era, $\Delta T(t)$, to the cumulative carbon emissions, $I_{em}(t)$,

$$\text{TCRE} = \frac{\Delta T(t)}{I_{em(t)}}. \tag{1}$$

The TCRE is usually considered for radiative forcing only from atmospheric CO_2, although this relationship may be generalised to include the effects of non-CO_2 radiative forcing [*Williams et al.*, 2016]. Two complementary views have been invoked to understand the TCRE. In the first view, emphasising the atmospheric response, the TCRE is explained in terms of the airborne fraction, $\Delta I_{atm}(t)/I_{em}(t)$, and the ratio of surface warming to changes in the atmospheric carbon inventory, $\Delta T(t)/\Delta I_{atm}(t)$ [*Matthews et al.*, 2009], which may be re-expressed in terms of a thermal contribution, $\Delta T(t)/R(t)$, the airborne fraction, and the ratio of radiative forcing and changes in the atmospheric carbon inventory, $R(t)/\Delta I_{atm}(t)$ [*Ehlert and Zickfeld*, 2017],

$$\text{TCRE} = \frac{\Delta T(t)}{\Delta I_{atm}(t)} \frac{\Delta I_{atm}(t)}{I_{em}(t)} = \frac{\Delta T(t)}{R(t)} \frac{R(t)}{\Delta I_{atm}(t)} \frac{\Delta I_{atm}(t)}{I_{em}(t)}. \tag{2}$$

This view of the TCRE may be further extended by connecting with the ocean heat uptake efficiency and the rate of emissions [*MacDougall and Friedlingstein*, 2015].

In the second view, emphasising the ocean response, the TCRE is interpreted as the product of a thermal contribution $\Delta T(t)/R(t)$, and a carbon contribution, $R(t)/I_{em}(t)$, [*Williams*

et al., 2016], which may be written in terms of the changes in the ocean carbon undersaturation, $\Delta I_{usat}(t)$, and terrestrial carbon, $\Delta I_{ter}(t)$, since the pre-industrial era [*Goodwin et al.*, 2015; *Williams et al.*, 2016, 2017a]:

$$\text{TCRE} = \frac{\Delta T(t)}{R(t)} \frac{R(t)}{I_{em}(t)} = \frac{\Delta T(t)}{R(t)} \frac{a}{I_B} \frac{(I_{em}(t) - \Delta I_{ter}(t) + \Delta I_{usat}(t))}{I_{em}(t)}, \tag{3}$$

here a is a CO_2 radiative forcing coefficient [*Myhre et al.*, 1998], I_B is the buffered carbon inventory and represents the effective available carbon in the combined atmosphere and ocean in the pre-industrial era [*Goodwin et al.*, 2007, 2009], $I_{usat}(t)$ is the ocean carbon undersaturation and measures how much carbon the entire ocean needs to take up to reach a carbon equilibrium with the atmosphere [*Goodwin et al.*, 2015], $I_{ter}(t)$ is the terrestrial carbon inventory and Δ represents the change since the pre-industrial era. The term $a(I_{em}(t) - \Delta I_{ter}(t))/I_B$ represents the part of the radiative forcing driven by the net carbon emissions to the combined atmosphere and ocean, while the term $a\Delta I_{usat}(t)/I_B$ represents the part of the radiative forcing driven by the excess amount of carbon in the atmosphere due to the ocean not being in carbon equilibrium with the atmosphere (see supplementary material).

In this study, we reconcile these two different perspectives of the TCRE. Our approach is to focus on the ratio of the changes in the ocean saturated carbon inventory, defined by how much carbon the ocean may take up relative to the instantaneous atmospheric CO_2, and the atmospheric carbon inventory. A new expression for the TCRE is provided including both the airborne fraction and the ocean saturated carbon inventory, which highlights the effect of carbonate chemistry in controlling the ratio of changes in ocean saturated and atmospheric carbon inventories (Section 2). This new TCRE expression is applied to understand the climate response during emissions and after emissions cease in a hierarchy of climate models: a box

model of the atmosphere-ocean and a realistic Earth system model (GFDL ESM2M) responding to a carbon emission over nearly 100 years and integrated for 1000 years [*Frölicher and Paynter*, 2015], and a suite of Earth system models integrated for a 1% annual rise in CO_2 for 140 years (Section 3).

2. Theory

2.1. A definition for the TCRE including the airborne fraction and ocean saturation

To understand the link between the two formulations of TCRE in (2) and (3), consider the changes in the global carbon inventory, where cumulative carbon emissions, $I_{em}(t)$, drive changes in the sum of the global carbon inventories for the atmosphere, $\Delta I_{atm}(t)$, ocean, $\Delta I_{ocean}(t)$, and terrestrial, $\Delta I_{ter}(t)$, systems relative to the pre-industrial era,

$$I_{em}(t) = \Delta I_{atm}(t) + \Delta I_{ocean}(t) + \Delta I_{ter}(t). \tag{4}$$

By connecting changes in the ocean carbon inventory, $\Delta I_{ocean}(t)$, to changes in the ocean saturated and ocean undersaturated components (defined relative to the instantaneous atmospheric CO_2), $\Delta I_{ocean}(t) = \Delta I_{sat}(t) - \Delta I_{usat}(t)$, then the carbon inventory changes in (4) may be rearranged as

$$I_{em}(t) - \Delta I_{ter}(t) + \Delta I_{usat}(t) = \Delta I_{atm}(t) + \Delta I_{sat}(t). \tag{5}$$

For the present day, the atmospheric CO_2 and the increase in the ocean carbon inventory, ΔI_{ocean}, are close to 400 ppm and 100 PgC, respectively, so that the increase in the saturated ocean carbon inventory, ΔI_{sat}, is about 900 PgC and in the ocean carbon undersaturation, ΔI_{usat}, is about 800 PgC.

Assuming that the changes in the radiative forcing, $R(t)$, are driven only by changes in atmospheric CO_2, the radiative forcing is expressed in terms of changes in either the net carbon emission to the combined atmosphere and ocean, $I_{em}(t) - \Delta I_{ter}(t)$, plus the ocean carbon undersaturation, $\Delta I_{usat}(t)$ [*Goodwin et al.*, 2015] (see supplementary material), or equivalently from (5), in the atmospheric, $\Delta I_{atm}(t)$, plus the ocean saturated carbon, $\Delta I_{sat}(t)$, inventories,

$$R(t) = \frac{a}{I_B}\left(I_{em}(t) - \Delta I_{ter}(t) + \Delta I_{usat}(t)\right) = \frac{a}{I_B}\left(\Delta I_{atm}(t) + \Delta I_{sat}(t)\right). \tag{6}$$

By substituting (6) into either (2) or (3), a new theoretical expression is derived for the TCRE,

$$\text{TCRE} = \frac{\Delta T(t)}{R(t)}\frac{a}{I_B}\left(\frac{\Delta I_{atm}(t) + \Delta I_{sat}(t)}{I_{em}(t)}\right) = \frac{\Delta T(t)}{R(t)}\frac{a}{I_B}\frac{\Delta I_{atm}(t)}{I_{em}(t)}\left(1 + \frac{\Delta I_{sat}(t)}{\Delta I_{atm}(t)}\right), \tag{7}$$

where the ratio $\Delta I_{sat}(t)/\Delta I_{atm}(t)$ represents the sensitivity of changes in the saturated ocean carbon inventory to changes in the atmospheric carbon inventory relative to the pre-industrial era. This new expression for the TCRE including the airborne fraction (7) is equivalent to the expression for the TCRE including ocean carbon undersaturation (3). Next, we explore how the ratio of the ocean saturated and atmospheric carbon inventories, $\Delta I_{sat}(t)/\Delta I_{atm}(t)$, is controlled by ocean carbonate chemistry.

2.2. Control of the ratio of the ocean saturated and atmospheric carbon inventories

In order to understand the evolution of the ratio $\Delta I_{sat}(t)/\Delta I_{atm}(t)$, consider an ocean buffer factor, $B(t)$, where the fractional changes in the atmospheric and ocean saturated carbon inventories are defined relative to the pre-industrial time, t_o, by

$$B(t) = \frac{\Delta I_{atm}(t)/I_{atm}(t_o)}{\Delta I_{sat}(t)/I_{sat}(t_o)}. \tag{8}$$

Rearranging (8), and drawing upon basic carbonate chemistry (see supplementary material), the ratio of the changes in the saturated ocean and atmospheric inventories, $\Delta I_{sat(t)}/\Delta I_{atm}(t)$, may be approximated by

$$\frac{\Delta I_{sat}(t)}{\Delta I_{atm}(t)} \approx \left(\frac{\rho_o V K_o}{M_a}\right)\left(\frac{K_1 K_2}{[H^+(z_s,t)]^2}\right)\left(\frac{CO_2(t)}{CO_2(t_o)}\right), \tag{9}$$

where M_a is the moles of gas in the atmosphere, ρ_o is a referenced ocean density, V is the ocean volume, and the hydrogen ion concentration, H^+, is evaluated at the sea surface, z_s. The changes in carbonate chemistry due to temperature are assumed relatively small compared with those changes due to atmospheric CO_2, and so the effect of changes in the solubility, K_o, and the equilibrium coefficients, K_1 and K_2, is neglected in (9).

In this approximation for the ratio $\Delta I_{sat(t)}/\Delta I_{atm}(t)$ in (9), each term has the following interpretation: the first term on the right hand side represents the value that this ratio would have if CO_2 was non-reactive in seawater; the second term is inversely associated with the abundance of H^+ ions in the ocean and decreases due to the increase in H^+ ions when there is an addition of CO_2 to seawater; and the third term is associated with the increase in the atmospheric CO_2 relative to its pre-industrial value. This approximation for $\Delta I_{sat}(t)/\Delta I_{atm}(t)$ is next used to understand the carbon control of the TCRE in a range of climate models (for the validity of this approximation, see the supplementary material).

3. Model assessment of the TCRE exploiting our theory and approximation

Our theory is used to interpret the control of the TCRE in a hierarchy of models forced by atmospheric CO_2 changes: a box model of the atmosphere-ocean system and an Earth system

model, both integrated for 1000 years, and a suite of Earth system models, integrated for 140 years.

3.1. Experimental design

The box model consists of three homogeneous layers: a well-mixed atmosphere, an ocean mixed layer with 100 m thickness, and an ocean interior with 3900 m thickness, all assumed to have the same horizontal area. The model solves for the heat and carbon exchange between these layers, including physical and chemical transfers, but ignoring biological transfers, and sediment and weathering interactions. The model is forced from an equilibrium by carbon emitted into the atmosphere with a constant rate of 20 PgC y^{-1} for 100 years and integrated for 1000 years. Ocean ventilation is represented by the ocean interior taking up the heat and carbon properties of the mixed layer on an e-folding time scale of 200 years (see supplementary material for the model closures). The radiative forcing, $R(t)$, varies according to the increase in atmospheric CO_2: $R(t) = a\Delta \ln CO_2(t)$ [*Myhre et al.*, 1998], where $a = 5.35$ W m^{-2} and the pre-industrial $CO_2(t_o)$ is 280 ppm. This radiative forcing, $R(t)$, is assumed to drive a global-mean radiative response, $\lambda(t)\Delta T(t)$, plus a planetary heat uptake, $N(t)$, such that $R(t) = \lambda(t)\Delta T(t) + N(t)$ [*Gregory et al.*, 2004; *Gregory and Forster*, 2008], where $\lambda(t)$ is the climate feedback parameter.

The response of an Earth system model is diagnosed over a 1000 years integration using the global coupled, carbon-climate model developed at Geophysical Fluid Dynamics Laboratory (GFDL-ESM2M) [*Dunne et al.*, 2012, 2013]. The idealised warming simulation experiment of *Frölicher and Paynter* [2015] is examined: forced by an annual 1% rise of atmospheric CO_2 until the global-mean surface warming reaches 2^oC at year 98 of the simulation; and then the

carbon emissions are set to zero. The non-CO_2 greenhouse gases are kept at their pre-industrial levels.

The climate responses during emissions are also assessed for a suite of other Earth system models forced by an annual 1% rise of atmospheric CO_2 for 140 years: CanESM2 [*Arora et al.*, 2011], HadGEM2-ES [*Jones et al.*, 2011], IPSL-CM5A-LR [*Dufresne et al.*, 2013], MPI-ESM-LR [*Giorgetta et al.*, 2013] and NorESM1-ME [*Tjiputra et al.*, 2013]. The selection of models samples the spread of responses within the CMIP5 models [*Williams et al.*, 2017b; *Goodwin et al.*, 2018].

3.2. Model diagnostics

3.2.1. Carbon inventory diagnostics

The atmosphere carbon inventory is estimated from atmospheric $CO_2(t)$, $I_{atm}(t) = M_a CO_2(t)$. The ocean carbon inventory is held as dissolved inorganic carbon, $I_{ocean}(t) = \rho_o V DIC(t)$, where $DIC(t)$ is the ocean volume-weighted dissolved inorganic carbon in mol C kg^{-1}. The atmosphere and ocean buffered carbon inventory is defined by $I_B = I_{atm}(t_o) + I_{sat}(t_o)/B_{rev}(t_o)$ [*Goodwin et al.*, 2007], where B_{rev} is the Revelle buffer factor [*Williams and Follows*, 2011]. The carbon inventories are further multiplied by 12 g mol^{-1} to be expressed in gC. The partitioning of dissolved inorganic carbon into bicarbonate, carbonate, and dissolved CO_2 is solved for using the algorithm of *Follows et al.* [2006].

The ocean saturated carbon inventory is estimated as $I_{sat}(t) = \rho_o V DIC_{sat}(t)$, where the saturated dissolved inorganic carbon, $DIC_{sat}(t)$, is diagnosed using the ocean potential temperature, salinity, alkalinity, and the atmospheric $CO_2(t)$ [*Ito and Follows*, 2005; *Lauderdale et al.*, 2013]. The saturated carbon inventory represents the amount of carbon the ocean would have if

the ocean reached a chemical equilibrium with the instantaneous atmospheric CO_2. The surface ocean equilibrates on an annual timescale with the atmosphere, so the surface dissolved CO_2 only slightly lags atmospheric CO_2. However, much of the ocean interior has not been in contact with the atmosphere since the pre-industrial era when the atmospheric CO_2 was 280 ppm. At present, atmospheric CO_2 is 400 ppm which corresponds to an increase in the ocean saturated carbon inventory relative to the pre-industrial era, ΔI_{sat}, of about 900 PgC. In comparison, the increase in the ocean carbon inventory relative to the pre-industrial era, ΔI_{ocean}, is about 100 PgC so that a further 800 PgC is needed for the ocean to become saturated to the present atmospheric CO_2.

3.2.2. Heat budget diagnostics

The planetary heat uptake, $N(t)$, is dominated by the ocean heat uptake [*Church et al.*, 2011]. In the box model, more than 95% of heat passes into the ocean; henceforth, we refer to the planetary and the ocean heat uptakes as being effectively equivalent. In the box model, the climate feedback parameter, λ, is assumed to be constant and equal to 1 W $m^{-2}K^{-1}$. In the Earth system models, the climate feedback parameter is more realistically taken to be time dependent, $\lambda(t)$ [*Senior and Mitchell*, 2000; *Armour et al.*, 2013; *Gregory and Andrews*, 2016]; $\lambda(t)$ is diagnosed from the radiative forcing, $R(t)$, the surface warming, $\Delta T(t)$, and the ocean heat uptake, $N(t)$, using the empirical heat budget, $R(t) = \lambda(t)\Delta T(t) + N(t)$ (see supplementary material). The equilibrium climate feedback parameter, λ_{eq}, is diagnosed at the end of the 1000 years model run in the GFDL-ESM2M model. For other Earth system models without long integrations, λ_{eq}, is taken from *Forster et al.* [2013] (Table 1 for net feedbacks).

In our diagnostics of the Earth system models, a 5 year filter is applied to remove higher frequency variability in the ocean heat uptake and surface warming, and diagnostics are not shown for the first 10 years when the cumulative emissions are still small and the climate response is controlled by internal variability.

3.3. Analysis and model responses

Our aim is to understand the climate response to carbon emissions in terms of the carbon and thermal contributions to the TCRE. The box model and the GFDL-ESM2M Earth system model, integrated over 1000 years, have broadly similar carbon and thermal responses, despite their different model complexity (Figures 1 and 3). The small differences between their model responses are associated with the more complex Earth system model having a time-varying climate feedback parameter, terrestrial carbon uptake, ocean circulation changes, and its carbon cycle including weathering and sediment interactions, and the effects of ocean biology. The suite of Earth system models reveal some inter-model variability, although their model responses are broadly similar to each other (Figures 2 and 3). Hence, the essential controls of the carbon and thermal contributions to the TCRE are similar in this range of climate models despite differences in model complexity. The details of the climate response are now worked through.

3.3.1. Carbon contribution

The carbon contribution to the TCRE from (6), $R(t)/I_{em}(t)$, is defined in terms of changes in the airborne fraction, $\Delta I_{atm}(t)/I_{em}(t)$, and the saturated oceanborne fraction, $\Delta I_{sat}(t)/I_{em}(t)$,

$$\frac{R(t)}{I_{em}(t)} = \frac{a}{I_B}\left(\frac{\Delta I_{atm}(t)}{I_{em}(t)} + \frac{\Delta I_{sat}(t)}{I_{em}(t)}\right) = \frac{a}{I_B}\frac{\Delta I_{atm}(t)}{I_{em}(t)}\left(1 + \frac{\Delta I_{sat}(t)}{\Delta I_{atm}(t)}\right). \tag{10}$$

In all the models, during emissions, there is an increase in the atmospheric carbon inventory, $\Delta I_{atm}(t)$, and in the ocean carbon inventory, $\Delta I_{ocean}(t)$, as some of the emitted carbon is transferred into the ocean (red and blue lines in Figure 1a and b). The rise in atmospheric CO_2 leads to an increase in the saturated ocean carbon inventory, $\Delta I_{sat}(t)$ (cyan lines in Figure 1a and b). After emissions cease, there is a decrease in the atmospheric inventory and the saturated ocean carbon inventory, accompanied by a further increase in the ocean carbon inventory.

These carbon inventory changes are often understood in terms of the airborne, oceanborne and landborne fractions of carbon, where $\Delta I_{atm}(t)/I_{em}(t) + \Delta I_{ocean}(t)/I_{em}(t) + \Delta I_{ter}(t)/I_{em}(t) = 1$ [*Jones et al.*, 2013]. The airborne fraction, $\Delta I_{atm}(t)/I_{em}(t)$, generally decreases as carbon is transferred from the atmosphere into the ocean until an equilibrium is approached in the box and the GFDL-ESM2M models (red lines in Figure 1c and d). The Earth system models experience large inter-model variability in terms of the magnitude of the airborne fraction (Figure 2a), with smaller airborne fraction associated with larger terrestrial carbon uptake. The trend in the airborne fraction, $\Delta I_{atm}(t)/I_{em}(t)$, is though similar in all the Earth system models: there is a rapid decrease in the airborne fraction over the first 50 years, followed by a slight increase, primarily associated with a slight decrease in the landborne fraction.

In all the models, there is also a decrease in the saturated oceanborne fraction, defined by $\Delta I_{sat}(t)/I_{em}(t)$ (cyan lines in Figure 1c and d, and coloured lines in Figure 2b). Hence, there is a decrease in the sum of the airborne and saturated oceanborne fractions, $(\Delta I_{atm}(t) + \Delta I_{sat}(t))/I_{em}(t)$ (black lines/shading in Figures 1c and d, and 3a, b and c), which is proportional to the carbon contribution, $R(t)/I_{em}(t)$, from (10). The rate of decrease in the saturated ocean-

borne fraction, $\Delta I_{sat}(t)/I_{em}(t)$, is different to that of the airborne fraction, $\Delta I_{atm}(t)/I_{em}(t)$, due to the effect of the carbonate chemistry.

The ratio of the changes in the saturated ocean and atmospheric carbon inventories, $\Delta I_{sat}(t)/\Delta I_{atm}(t)$, is controlled by the carbonate chemistry: $\Delta I_{sat}(t)/\Delta I_{atm}(t)$ is proportional to $(K_1K_2/[H^+(z_s,t)]^2)(CO_2(t)/CO_2(t_o))$ from (9). The magnitude and time variability of the ratio $\Delta I_{sat}(t)/\Delta I_{atm}(t)$ is similar in all the models (black lines in Figure 1e and f, and coloured lines in Figure 2c). During emissions, the ratio $\Delta I_{sat}(t)/\Delta I_{atm}(t)$ decreases (black lines in Figure 1e and f) from the increase in H^+ ions (red dashed lines in Figure 1e and f) despite the accompanying increase in atmospheric CO_2 (red dashed-doted lines in Figure 1e and f). After emissions cease, the ratio $\Delta I_{sat}(t)/\Delta I_{atm}(t)$ increases due to the decrease in H^+ ions, dominating over the effect of the decrease in atmospheric CO_2. In comparison, if the effect of carbonate chemistry is artificially excluded, the ratio $\Delta I_{sat}(t)/\Delta I_{atm}(t)$ is constant and equal to $\rho_o V K_o/M_a$ (red dotted lines in Figure 1e and f).

3.3.2. Thermal contribution

The thermal contribution to the TCRE, $\Delta T(t)/R(t)$, is understood via the empirical heat budget [*Gregory et al.*, 2004; *Gregory and Forster*, 2008], where radiative forcing drives a radiative response and a heat uptake, $R(t) = \lambda(t)\Delta T(t) + N(t)$, which may be re-expressed as

$$\frac{\Delta T(t)}{R(t)} = \frac{1}{\lambda_{eq}}\left[\frac{\lambda_{eq}}{\lambda(t)}\left(1 - \frac{N(t)}{R(t)}\right)\right], \tag{11}$$

where the term in the square brackets is the realised-warming fraction [*Solomon et al.*, 2009; *Frölicher et al.*, 2014; *Frölicher and Paynter*, 2015] (red lines/shading in Figure 3a, b and c).

In the box model, the realised-warming fraction, $(\lambda_{eq}/\lambda(t))(1 - N(t)/R(t))$, is driven by the fraction of the radiative forcing that warms the surface versus the fraction used to increase

ocean heat content, $N(t)/R(t)$. In the Earth system models, the time variation of $\lambda(t)$ also affects the realised-warming fraction. Initially, in all the models, most of the radiative forcing is used to drive ocean heat uptake and warming of the ocean interior. As the ocean interior becomes warmer, gradually a smaller fraction of the radiative forcing warms the ocean interior and the realised-warming fraction increases (red lines/shading in Figure 3a, b and c). The large decline of the realised-warming fraction in the GFDL-ESM2M model during the first 20 years is associated with an initial large increase in $\lambda(t)$.

3.3.3. Transient Climate Response to Carbon Emissions

The TCRE may be defined in terms of a product of thermal and carbon contributions by combining (7) and (11),

$$\text{TCRE} = \frac{a}{\lambda_{eq} I_B} \left[\frac{\lambda_{eq}}{\lambda(t)} \left(1 - \frac{N(t)}{R(t)} \right) \right] \left[\frac{\Delta I_{atm}(t)}{I_{em}(t)} \left(1 + \frac{\Delta I_{sat}(t)}{\Delta I_{atm}(t)} \right) \right], \tag{12}$$

where the time-independent term, $a/(\lambda_{eq} I_B)$, is the long-term equilibrium climate response to emissions [*Williams et al.*, 2012], and the terms in the square brackets represent the non-dimensional, time-dependent thermal and carbon contributions to the TCRE.

Our theoretical relationship for the TCRE diagnosed from (12) agrees well with the actual TCRE diagnosed from (1) for both the box and the GFDL-ESM2M models integrated for 1000 years (compare the black and blue lines in Figure 3d and e); this agreement also holds for the other Earth system models integrated for 140 years (see supplementary material).

The TCRE is viewed as a product of the thermal and the carbon contributions. The carbon contribution follows the decrease in $(\Delta I_{atm}(t)/I_{em}(t))(1+\Delta I_{sat}(t)/\Delta I_{atm}(t))$, while the thermal contribution follows the increase in the realised-warming fraction, $(\lambda_{eq}/\lambda(t))(1-N(t)/R(t))$ (Figure 3a, b and c). Thus, the thermal contribution acts to increase the TCRE, while the

carbon contribution acts to decrease the TCRE. The TCRE is constant when changes in these thermal and carbon contributions compensate for each other. However, in all the models, during emissions, there is a general decrease in the TCRE after about the first 30 years, with the rate of the decrease being model dependent (Figure 3d, e and f). After emissions cease, there is an increase in the TCRE in the box model and the GFDL-ESM2M (Figure 3d and e).

To gain further insight, now combine (9) and (12) to obtain a TCRE expression based on our carbonate approximation,

$$\text{TCRE} \approx \frac{a}{\lambda_{eq} I_B}\left[\frac{\lambda_{eq}}{\lambda(t)}\left(1-\frac{N(t)}{R(t)}\right)\right]\left[\frac{\Delta I_{atm}(t)}{I_{em}(t)}\left(1+\frac{\rho_o V K_o}{M_a}\frac{K_1 K_2}{[H^+(z_s,t)]^2}\frac{CO_2(t)}{CO_2(t_o)}\right)\right]. \quad (13)$$

This carbonate approximation for the TCRE underestimates the TCRE in the box model and overestimates the TCRE in the Earth system models, but captures its variability in time in all the models (compare the black and red lines in Figure 3d and e, for the suite of Earth system models see the supplementary material).

If the effect of carbonate chemistry is artificially excluded in (13), the contribution to the TCRE from $(a/(\lambda(t)I_B))(1-N(t)/R(t))(\Delta I_{atm}(t)/I_{em}(t))(1+\rho_o V K_o/M_a)$ is nearly constant (dashed lines in Figure 3d, e and f); in the Earth system models, there is though a slight increase in the TCRE without the explicit effect of the carbonate chemistry after about the first 20 years from the temporal evolution of $\lambda(t)$, changes in ocean circulation, and changes in terrestrial carbon uptake. If the effect of carbonate chemistry is now included in (13), the term involving carbonate chemistry, $(K_1K_2/[H^+(z_s,t)]^2)(CO_2(t)/CO_2(t_o))$, increases the magnitude of the TCRE, and modulates the carbon contribution to the TCRE in a consistent manner in all the models. Hence, the carbonate chemistry leads to a long-term decrease in the TCRE during emissions and an increase in the TCRE after emissions cease (Figure 3d, e and f).

4. Conclusions

The Transient Climate Response to Emissions (TCRE) is a fundamental climate metric, measuring the surface warming increase for a cumulative carbon emission [*Matthews et al.*, 2009; *Gillet et al.*, 2013]. While the TCRE may simply be diagnosed from output of climate model projections, theory may be exploited to understand how the TCRE is controlled in terms of physical and biogeochemical mechanisms [*Goodwin et al.*, 2015; *MacDougall and Friedlingstein*, 2015; *Williams et al.*, 2016, 2017a]. Our new expression for the TCRE involves a product of two time-varying thermal and carbon contributions: the thermal contribution involves ocean heat uptake and the climate feedback parameter; and the carbon contribution involves the airborne fraction (depending on ocean and terrestrial carbon uptake) and the ratio of ocean saturated and atmospheric carbon inventories (depending on ocean carbonate chemistry).

Our viewpoint of how the TCRE is controlled is assessed using a hierarchy of climate models: a box model of the atmosphere-ocean and an Earth system model, both diagnosed for integrations for 1000 years, and a suite of Earth system models diagnosed over 140 years. For all models, there is the same ocean carbonate chemistry response: during emissions, an increase in acidity at the ocean surface leads to a decrease in the ratio of the ocean saturated and atmospheric carbon inventories, which decreases the carbon contribution to the TCRE; and after emissions cease, a decrease in acidity at the ocean surface leads to an increase in this ratio and an increase in the carbon contribution to the TCRE.

The TCRE need not remain constant in time [*Krasting et al.*, 2014] due to changes in the time-dependent thermal and carbon contributions. While the ocean ventilated heat and carbon uptake may act in a nearly compensating manner [*Solomon et al.*, 2009], the carbonate chemistry leads

to a systematic decrease in the TCRE with increasing acidity. If the effect of the carbonate chemistry is artificially excluded in the climate model, the TCRE is smaller in magnitude and is nearly constant in time due to the compensating effects of ocean heat and carbon uptake from ventilation.

In summary, ocean carbonate chemistry is important in controlling the magnitude of the TCRE and contributing to its temporal evolution. Reassuringly, in a range of climate models with differing complexity, carbonate chemistry provides a similar control of the carbon contribution to the TCRE. Inter-model differences in the TCRE are more likely due to other factors [*Williams et al.*, 2017b], such as the thermal contribution to the TCRE, involving the climate feedback parameter and ocean ventilation of heat, or the separate carbon contribution to the TCRE from the airborne fraction, altered by ocean ventilation of carbon and terrestrial cycling of carbon.

Acknowledgement

This work was supported by a UK Natural Environmental Research Council grant NE/N009789/1. We thank Thomas Frölicher for providing outputs for the idealised warming simulation experiment using the GFDL-ESM2M model. We also thank two referees for constructive comments and feedback. We also acknowledge the World Climate Research Programmes Working Group on Coupled Modelling responsible for CMIP that provided access to the outputs from the Earth system models. The computer code for the box model is provided in the supplementary material and the basic model data sets for the GFDL-ESM2M are available via the British Ocean Data Centre data portal (https://www.bodc.ac.uk/resources/inventories/edmed/report/6712/).

References

Allen, M. R., D. J. Frame, C. Huntingford, C. D. Jones, J. A. Lowe, M. Meinshausen, and N. Meinshausen, Warming caused by cumulative carbon emissions towards the trillionth tonne, *Nature*, *458*, 1163–1166, doi:10.1038/nature08019, 2009.

Armour, K. C., C. M. Bitz, and G. H. Roe, Time-varying climate sensitivity from regional feedbacks, *Journal of Climate*, *26*(13), 4518–4534, doi:10.1175/JCLI-D-12-00544.1, 2013.

Arora, V. K., J. F. Scinocca, G. J. Boer, J. R. Christian, K. L. Denman, G. M. Flato, V. V. Kharin, W. G. Lee, and W. J. Merryfield, Carbon emission limits required to satisfy future representative concentration pathways of greenhouse gases, *Geophysical Research Letters*, *38*(5), L05,805, doi:10.1029/2010GL046270, 2011.

Church, J. A., et al., Revisiting the Earth's sea-level and energy budgets from 1961 to 2008, *Geophysical Research Letters*, *38*(18), L18,601, doi:10.1029/2011GL048794, 2011.

Dufresne, J.-L., M. A. Foujols, S. Denvil, et al., Climate change projections using the IPSL-CM5 Earth system model: from CMIP3 to CMIP5, *Climate Dynamics*, *40*, 21232165, doi: 10.1007/s00382-012-1636-1, 2013.

Dunne, J. P., et al., GFDL's ESM2 global coupled climate carbon Earth system models. Part I: Physical formulation and baseline simulation characteristics, *Journal of Climate*, *25*(19), 6646–6665, doi:10.1175/JCLI-D-11-00560.1, 2012.

Dunne, J. P., et al., GFDL's ESM2 global coupled climate carbon Earth system models. Part II: Carbon system formulation and baseline simulation characteristics, *Journal of Climate*, *26*(7), 2247–2267, doi:10.1175/JCLI-D-12-00150.1, 2013.

Ehlert, D., and K. Zickfeld, What determines the warming commitment after cessation of CO_2 emissions, *Environmental Research Letters*, *12*, 015,002, doi:https://doi.org/10.1088/1748-9326/aa564a, 2017.

Follows, M. J., T. Ito, and S. Dutkiewicz, On the solution of the carbonate chemistry system in ocean biogeochemistry models, *Ocean Modelling*, *12*, 290–301, doi:https://doi.org/10.1016/j.ocemod.2005.05.004, 2006.

Forster, P. M., T. Andrews, P. Good, J. M. Gregory, L. S. Jackson, and M. Zelinka, Evaluating adjusted forcing and model spread for historical and future scenarios in the CMIP5 generation of climate models, *Journal of Geophysical Research: Atmospheres*, *118*(3), 1139–1150, doi:10.1002/jgrd.50174, 2013.

Frölicher, T. L., and D. J. Paynter, Extending the relationship between global warming and cumulative carbon emissions to multi-millennial timescales, *Environmental Research Letters*, *10*, 075,002, doi:10.1088/1748-9326/10/7/075002, 2015.

Frölicher, T. L., M. Winton, and J. L. Sarmiento, Continued global warming after CO_2 emissions stoppage, *Nature Climate Change*, *4*, 40–44, doi:10.1038/nclimate2060, 2014.

Gillet, N. P., V. K. Arora, D. Matthews, and M. R. Allen, Constraining the ratio of global warming to cumulative CO_2 emissions using CMIP5 simulations, *Journal of Climate*, *26*, 6844–6858, doi:10.1175/JCLI-D-12-00476.1, 2013.

Giorgetta, M. A., et al., Climate and carbon cycle changes from 1850 to 2100 in MPI-ESM simulations for the Coupled Model Intercomparison Project phase 5, *Journal of Advances in Modeling Earth Systems*, *5*(3), 572–597, doi:10.1002/jame.20038, 2013.

Goodwin, P., R. G. Williams, M. J. Follows, and S. Dutkiewicz, Ocean-atmosphere partitioning of anthropogenic carbon dioxide on centennial timescales, *Global Biogeochemical Cycles*, *21*(1), GB1014, doi:10.1029/2006GB002810, 2007.

Goodwin, P., R. G. Williams, R. G. Ridgwell, and M. J. Follows, Climate sensitivity to the carbon cycle modulated by past and future changes to ocean chemistry, *Nature Geoscience*, *2*, 145–150, doi:10.1038/ngeo416, 2009.

Goodwin, P., R. G. Williams, and A. Ridgwell, Sensitivity of climate to cumulative carbon emissions due to compensation of ocean heat and carbon uptake, *Nature Geoscience*, *8*, 29–34, doi:10.1038/ngeo2304, 2015.

Goodwin, P., A. Katavouta, V. M. Roussenov, G. L. Foster, E. J. Rohling, and R. G. Williams, Pathways to 1.5^{o}C and 2^{o}C warming based on observational and geological constraints, *Nature Geoscience*, *11*, 102–107, doi:10.1038/s41561-017-0054-8, 2018.

Gregory, J. M., and T. Andrews, Variation in climate sensitivity and feedback parameters during the historical period, *Geophysical Research Letters*, *43*(8), 3911–3920, doi:10.1002/2016GL068406, 2016.

Gregory, J. M., and P. M. Forster, Transient climate response estimated from radiative forcing and observed temperature change, *Journal of Geophysical Research: Atmospheres*, *113*, D23,105, doi:10.1029/2008JD010405, 2008.

Gregory, J. M., W. J. Ingram, M. A. Palmer, G. S. Jones, P. A. Stott, R. B. Thorpe, J. A. Lowe, T. C. Johns, and K. D. Williams, A new method for diagnosing radiative forcing and climate sensitivity, *Geophysical Research Letters*, *31*(3), L03,205, doi:10.1029/2003GL018747, 2004.

Ito, T., and M. J. Follows, Preformed phosphate, soft tissue pump and atmospheric CO_2, *Journal of Marine Research*, *63*, 813–839, doi:https://doi.org/10.1357/0022240054663231, 2005.

Jones, C., et al., Twenty-first-century compatible CO_2 emissions and airborne fraction simulated by CMIP5 Earth System models under four Representative Concentration Pathways, *Journal of Climate*, *26*(13), 4398–4413, doi:10.1175/JCLI-D-12-00554.1, 2013.

Jones, C. D., et al., The HadGEM2-ES implementation of CMIP5 centennial simulations, *Geoscientific Model Development*, *4*(3), 543–570, doi:10.5194/gmd-4-543-2011, 2011.

Krasting, J. P., J. P. Dunne, E. Shevliakova, and R. J. Stouffer, Trajectory sensitivity of the transient climate response to cumulative carbon emissions, *Geophys. Res. Lett.*, *41*, 2520–2527, doi:10.1002/2013GL059141, 2014.

Lauderdale, J. M., A. C. N. Garabato, K. I. C. Oliver, M. J. Follows, and R. G. Williams, Wind-driven changes in southern ocean residual circulation, ocean carbon reservoirs and atmospheric CO_2, *Climate Dynamics*, *41*, 2145–2164, doi:https://doi.org/10.1007/s00382-012-1650-3, 2013.

MacDougall, A. H., and P. Friedlingstein, The origin and limits of the near proportionality between climate warming and cumulative CO_2 emissions, *Journal of Climate*, *28*(10), 4217–4230, doi:10.1175/JCLI-D-14-00036.1, 2015.

Matthews, H. D., N. P. Gillett, P. A. Stott, and K. Zickfeld, The proportionality of global warming to cumulative carbon emissions, *Nature*, *459*, 829–833, doi:10.1038/nature08047, 2009.

Myhre, G., E. J. Highwood, K. P. Shine, and F. Stordal, New estimates of radiative forcing due to well mixed greenhouse gases, *Geophysical Research Letters*, *25*, 2715–2718, doi:10.1029/98GL01908, 1998.

Senior, C. A., and J. F. B. Mitchell, The time-dependence of climate sensitivity, *Geophysical Research Letters*, *27*(17), 2685–2688, doi:10.1029/2000GL011373, 2000.

Solomon, S., G.-K. Plattner, R. Knutti, and P. Friedlingstein, Irreversible climate change due to carbon dioxide emissions, *Proc. Natl. Acad. Sci. USA*, *106*, 1704–1709, doi: 10.1073/pnas.0812721106, 2009.

Tjiputra, J. F., C. Roelandt, M. Bentsen, D. M. Lawrence, T. Lorentzen, J. Schwinger, Ø. Seland, and C. Heinze, Evaluation of the carbon cycle components in the Norwegian Earth system model (NorESM), *Geoscientific Model Development*, *6*(2), 301–325, doi:10.5194/gmd-6-301-2013, 2013.

Williams, R. G., and M. J. Follows, *Ocean Dynamics and the Carbon Cycle: Principles and Mechanisms*, 416 pp., Cambridge University Press, 2011.

Williams, R. G., P. Goodwin, A. Ridgwell, and P. L. Woodworth, How warming and steric sea level rise relate to cumulative carbon emissions, *Geophysical Research Letters*, *39*, L19,715, doi:10.1029/2012GL052771, 2012.

Williams, R. G., P. Goodwin, V. M. Roussenov, and L. Bopp, A framework to understand the Transient Climate Response to Emissions, *Environmental Research Letters*, *11*, doi: 10.1088/1748-9326/11/1/015003, 2016.

Williams, R. G., V. Roussenov, T. L. Frölicher, and P. Goodwin, Drivers of continued surface warming after the cessation of carbon emissions, *Geophysical Research Letters*, *44*, 10,63310,642, doi:10.1002/2017GL075080, 2017a.

Williams, R. G., V. Roussenov, P. Goodwin, L. Resplandy, and L. Bopp, Sensitivity of global warming to carbon emissions: Effects of heat and carbon uptake in a suite of Earth system

models, *Journal of Climate*, *30*(23), 9343–9363, doi:10.1175/JCLI-D-16-0468.1, 2017b.

Zickfeld, K., M. Eby, H. D. Matthews, and A. J. Weaver, Setting cumulative emissions targets to reduce the risk of dangerous climate change, *Proc. Natl. Acad. Sci. USA*, *106*, 16,129–16,134, doi:10.1073/pnas.0805800106, 2009.

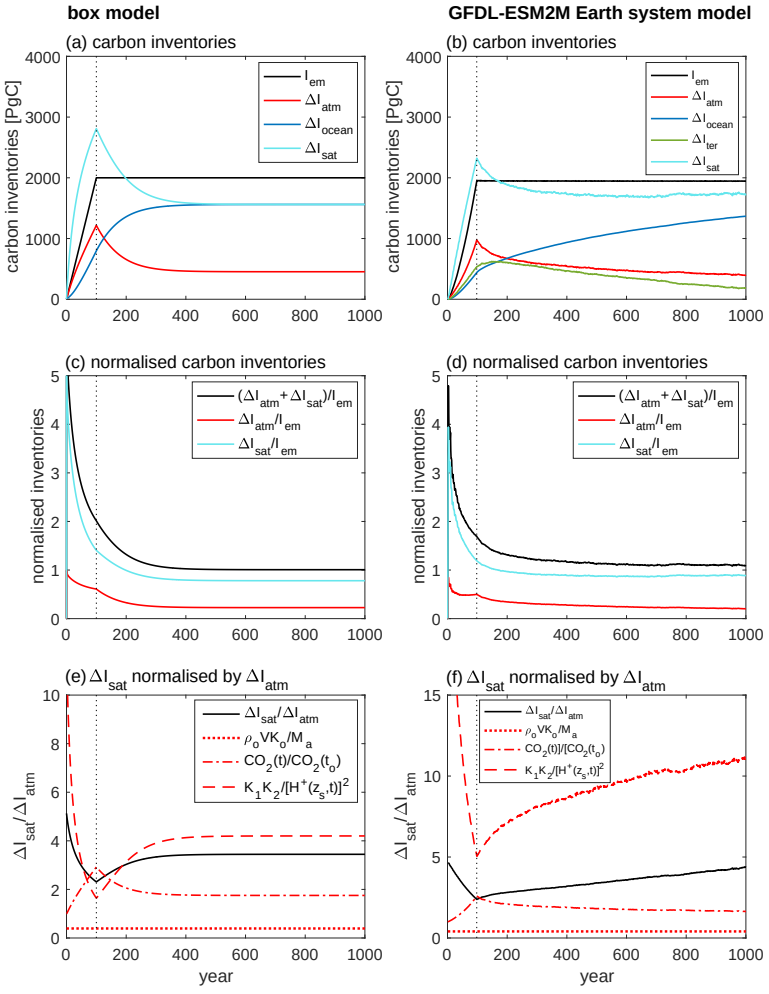

Figure 1. Carbon response for the box model (left panels) and the GFDL-ESM2M Earth system model (right panels) integrated for 1000 years: (a), (b) cumulative carbon emissions, $I_{em}(t)$, along with the carbon inventory changes relative to the pre-industrial era for the atmosphere, $\Delta I_{atm}(t)$, the ocean, $\Delta I_{ocean}(t)$, the terrestrial system, $\Delta I_{ter}(t)$, and the ocean saturated carbon, $\Delta I_{sat}(t)$; (c), (d) the airborne fraction, $\Delta I_{atm}(t)/I_{em}(t)$, the oceanborne fraction for saturated carbon, $\Delta I_{sat}(t)/I_{em}(t)$), and their sum, $(\Delta I_{atm}(t)+\Delta I_{sat}(t))/I_{em}(t)$; and (e), (f) the ratio of the changes in the saturated ocean and atmospheric carbon inventories, $\Delta I_{sat}(t)/\Delta I_{atm}(t)$, along with the three terms that control this ratio from (9): $\rho_o V K_o/M_a$, $CO_2(t)]/CO_2(t_o)$ and $K_1K_2/[H^+(z_s,t)]^2$. The thin black dotted line notes the cessation of the emissions.

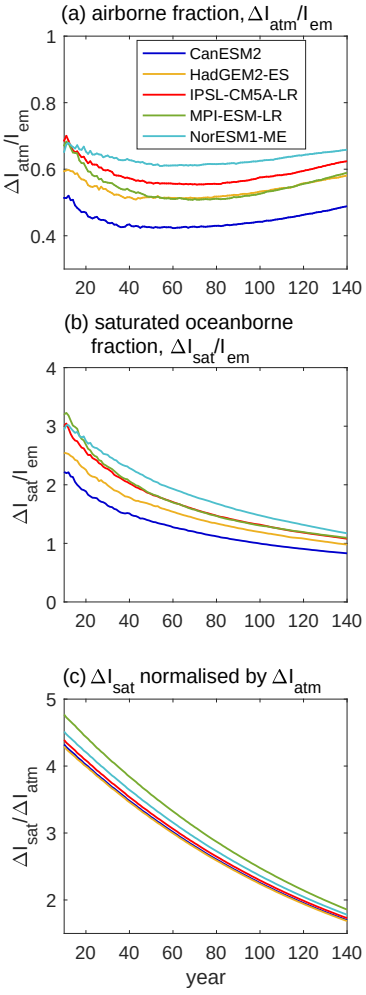

Figure 2. Carbon response for the suite of Earth system models integrated for 140 years: (a) the airborne fraction, $\Delta I_{atm}(t)/I_{em}(t)$; (b) the oceanborne fraction for saturated carbon, $\Delta I_{sat}(t)/I_{em}(t)$); and (c) the ratio of the changes in the saturated ocean and atmospheric carbon inventories, $\Delta I_{sat}(t)/\Delta I_{atm}(t)$.

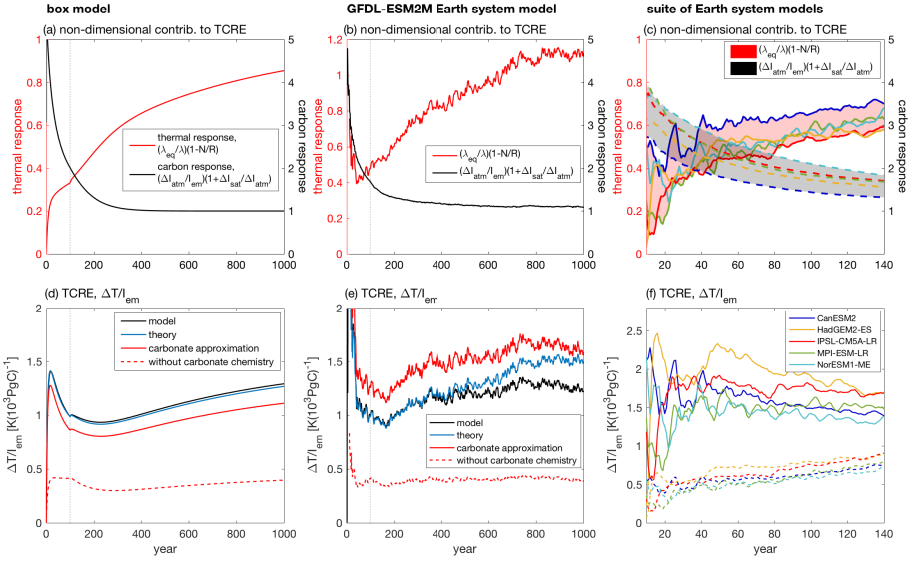

Figure 3. TCRE for the box model (left panels) and the GFDL-ESM2M Earth system model (middle panels), integrated for 1000 years, and the suite of Earth system models (right panels), integrated for 140 years: (a), (b), (c) the non-dimensional, thermal contribution, $(\lambda_{eq}/\lambda(t))(1-N(t)/R(t))$, and carbon contribution, $(\Delta I_{atm}(t)/\Delta I_{em}(t))(1+\Delta I_{sat}(t)/\Delta I_{atm}(t))$, to the TCRE; (d), (e) the TCRE diagnosed from (1) (black lines), using our theory from (12) (blue lines) and using the carbonate approximation from (13) (red lines) for the box and the GFDL-ESM2M models; and (f) the TCRE diagnosed from (1) (solid lines), for the suite of Earth system models. In addition, estimates of the TCRE by artificially excluding the effect of the carbonate chemistry in (13) are denoted in (d), (e) and (f) by dashed lines. The thin black dotted line notes the cessation of the emissions.